Estimation of Respiratory Rate From Photoplethysmogram Data Using Time–Frequency Spectral Estimation

Ki H. Chon*, *Senior Member, IEEE*, Shishir Dash, and Kihwan Ju

***Abstract*—We present a new method that uses the pulse oximeter signal to estimate the respiratory rate. The method uses a recently developed time–frequency spectral estimation method, variable-frequency complex demodulation (VFCDM), to identify frequency modulation (FM) of the photoplethysmogram waveform. This FM has a measurable periodicity, which provides an estimate of the respiration period. We compared the performance of VFCDM to the continuous wavelet transform (CWT) and autoregressive (AR) model approaches. The CWT method also utilizes the respiratory sinus arrhythmia effect as represented by either FM or AM to estimate respiratory rates. Both CWT and AR model methods have been previously shown to provide reasonably good estimates of breathing rates that are in the normal range (12–26 breaths/min). However, to our knowledge, breathing rates higher than 26 breaths/min and the real-time performance of these algorithms are yet to be tested. Our analysis based on 15 healthy subjects reveals that the VFCDM method provides the best results in terms of accuracy (smaller median error), consistency (smaller interquartile range of the median value), and computational efficiency (less than 0.3 s on 1 min of data using a MATLAB implementation) to extract breathing rates that varied from 12–36 breaths/min.**

***Index Terms*—FM, pulse oximeter, respiratory sinus arrhythmia, time–frequency analysis.**

I. Introduction

FOR patients at risk of cardiorespiratory failure, it is important to monitor the efficiency of gas exchange in the lungs, i.e., how well the arterial blood is oxygenated [1]. A noninvasive means to monitor arterial oxygen saturation (SaO_2) on a continuous basis is pulse oximetry, a well-established technology based on photoplethysmography (PPG) that has become one of the most commonly used patient monitors during anesthesia and in intensive care units. Its popularity stems from the fact that the pulse oximeter can be used to noninvasively measure both SaO_2 and basic cardiac function (e.g., heart rhythms). Furthermore, it is simple to operate and does not discomfort patients.

Given the ubiquity and simplicity of pulse oximetry, it is desirable to maximize its potential by exploring additional measurements that we can derive from the pulse oximeter. Extraction of respiratory rate from pulse oximetry data is one example, as the signal from the pulse oximeter contains not only the heart beat but also a respiratory signal. Respiratory rate is important for many clinical uses including detecting sleep apnea [2], sudden infant death syndrome [3], and chronic obstructive pulmonary disease [4], and measurements of respiratory rate are indicated in many intensive care and operative settings. The current standard practice for the automatic measurement of respiration rate requires monitoring of CO_2 production using a capnograph, which is an expensive device that requires a significant amount of maintenance. In addition, it requires a mask or nasal cannula, and is therefore obtrusive to the patient and cumbersome to use. Obtaining accurate respiratory rates from a pulse oximeter in addition to SaO_2 and heart rate is very appealing from both economic and patient comfort perspectives.

The reason why many researchers feel that it is possible to obtain respiratory rate from the PPG signal is due to evidence that the respiration rate modulates both amplitude and frequency of the signal [5]–[8]. This phenomenon is similar to the respiratory sinus arrhythmia modulating the heart rate signal. Thus, this suggests that the respiratory rate can be obtained by detecting the presence of AM and FM. However, detection of these modulations is often difficult, due to myriad causes [9]–[11]. Three primary culprits stand out: 1) the time-varying (TV) nature of these modulations; 2) both AM and FM are often subtle, and thus, the highest possible time and frequency resolutions are needed to detect them; and 3) the presence of motion and noise artifacts can mask AM and FM.

To this end, many recent efforts using advanced signal processing algorithms to overcome the aforementioned problems have shown tantalizing potential. Using a series of adaptive low-pass filters (LPFs) followed by high-pass filters with suitable cutoff frequencies, Nakajima *et al.* [9] were able to show that heart and respiratory signals can be distinguished in the PPG signal. However, this technique's accuracy degrades with motion artifacts, which are especially prevalent in the PPG signal during exercise. Furthermore, the cutoff frequencies of the low- and high-pass filters need to be tailored to individuals, which preclude wide clinical use. With the recent introduction of new techniques using estimation of time–frequency spectra (TFS) for analyzing nonstationary signals, there is at last the promise of succeeding at our goal. In this category, several studies have utilized short-time Fourier transform (STFT) [8] and continuous wavelet transform (CWT) [5]–[7], [12]–[14] to extract the respiratory rate from the PPG signal. However, success is predicated

Manuscript received November 24, 2008; revised February 9, 2009. First published April 14, 2009; current version published July 15, 2009. This work was supported in part by the Office of Naval Research Work Unit under Grant N00014-08-1-0244. *Asterisk indicates corresponding author.*

*K. H. Chon is with the Department of Biomedical Engineering, State University of New York (SUNY) at Stony Brook, Stony Brook, NY 11794 USA (e-mail: ki.chon@sunysb.edu).

S. Dash and K. Ju are with the Department of Biomedical Engineering, State University of New York (SUNY) at Stony Brook, Stony Brook, NY 11794 USA (e-mail: sdash@ic.sunysb.edu; kihwanju@hotmail.com).

Color versions of one or more of the figures in this paper are available online at http://ieeexplore.ieee.org.

Digital Object Identifier 10.1109/TBME.2009.2019766

on obtaining the highest possible time and frequency resolution, which is impossible with either the STFT or the CWT. It is widely known that the CWT cannot simultaneously provide high resolution in time and high resolution in frequency. Generally, CWTs provide high resolution in frequency only at low frequencies and high time resolution only at high frequencies. For subjects with chronic obstructive pulmonary disease, reflection of respiratory rate via the AM and FM of the PPG signal is often subtle as these subjects are physically limited from breathing in a normal manner. It is unclear what is considered "LF" because the LF range can vary depending on the dynamics of the system. Furthermore, real-time implementation is especially challenging for the CWT. The studies by Leonard *et al.* [5]–[7], Addison and Watson [12], [13], and Clifton *et al.* [14] show relatively good results; however, the CWT is impractical because the extraction of respiratory rate is done in some cases with the use of FM while in other cases with the AM of heart rate. This is clearly a difficult situation since it would require additional adaptive decision-making schemes to determine when to use either FM or AM of the heart rate signal to extract respiratory rates.

Recently, a method based on autoregressive (AR) modeling has been proposed, claiming to provide more accurate results than the existing techniques [15]. While the method is easy to implement, this approach is also problematic because the AR model order needs to be tuned to an individual, or at best, to specific age groups and/or for specific time periods studied. For example, the AR model requires different sets of modeling parameters for 5 min and 30 s data, respectively. Furthermore, a separate threshold criterion is needed to identify poles with the highest magnitude as there can be multiple poles meeting the specifications.

To improve upon the limitations of current techniques, the goal of this paper is the application of a new algorithm that we have recently developed [16], which is able to accurately extract continuous respiratory rate from noninvasive recordings of PPG signals. The algorithm is based on one of the highest possible time and frequency resolution approaches to estimating TFS and associated amplitudes via the use of variable-frequency complex demodulation (VFCDM) [16]. The VFCDM provides the best time and frequency resolution and most accurate amplitude estimates when compared to the smoothed pseudo-Wigner–Ville, CWT, and Hilbert–Huang transform methods [16]. Thus, it is expected that the VFCDM algorithm will be more accurate than the power spectral density, CWT, and other time–frequency-based methods for determining respiratory rate. Indeed, with this implementation, we are able to accurately extract wide ranges of respiratory rates from the raw PPG signals. The VFCDM method was tested on 15 different subjects for breathing frequencies ranging from 0.2 to 0.6 Hz. Results were compared to the CWT method [5]–[7], [12]–[14] and an AR method [15], which have been shown to be among the best existing techniques for extracting breathing rate information from PPG signals.

II. Methods

A. Algorithm Development

The VFCDM method has been published and tested with different physiological signals [16]–[18], and thus, will be briefly summarized. For further details than what is provided in this section, see [16].

1) VFCDMs for Estimation of TFS: The VFCDM method involves a two-step procedure. The first step is to use the complex demodulation (CDM) or what we termed the fixed-frequency CDM (FFCDM) to obtain an estimate of the TFS, and the second step is to select only the dominant frequencies of interest for further refinement of the time–frequency resolution using the VFCDM approach. In the first step of the VFCDM method, a bank of LPFs is used to decompose the signal into a suite of band-limited signals. The analytic signals that are obtained from these, through use of the Hilbert transform, then provide estimates of instantaneous amplitude, frequency, and phase within each frequency band. Consider a sinusoidal signal $x(t)$ to be a narrow-band oscillation with a center frequency f_0, instantaneous amplitude $A(t)$, phase $\phi(t)$, and the direct current component $\mathrm{dc}(t)$ defined as

$$x(t) = \mathrm{dc}(t) + A(t)\cos\left(2\pi f_0 t + \phi(t)\right). \tag{1}$$

For a given center frequency, we can extract the instantaneous amplitude information $A(t)$ and phase information $\phi(t)$ by multiplying (1) by $e^{-j2\pi f_0 t}$, which results in the following:

$$\begin{aligned} z(t) &= x(t)e^{-j2\pi f_0 t} \\ &= \mathrm{dc}(t)e^{-j2\pi f_0 t} + \left(\frac{A(t)}{2}\right)e^{j\phi(t)} \\ &\quad + \left(\frac{A(t)}{2}\right)e^{-j(4\pi f_0 t + \phi(t))}. \end{aligned} \tag{2}$$

A leftward shift by $e^{-j2\pi f_0 t}$ moves the center frequency f_0 to zero frequency in the spectrum of $z(t)$. If $z(t)$ in (2) is subjected to an ideal LPF with a cutoff frequency $f_c < f_0$, then the filtered signal $z_{\mathrm{lp}}(t)$ will contain only the component of interest, and we obtain the following:

$$z_{\mathrm{lp}}(t) = \left(\frac{A(t)}{2}\right)e^{j\phi(t)} \tag{3}$$

$$A(t) = 2\left|z_{\mathrm{lp}}(t)\right| \tag{4}$$

$$\phi(t) = \tan^{-1}\left(\frac{\mathrm{Im}(z_{\mathrm{lp}}(t))}{\mathrm{Re}(z_{\mathrm{lp}}(t))}\right). \tag{5}$$

Consider a case when a modulating frequency is not fixed as described before but varies as a function of time. In this case, the signal $x(t)$ can be written in the following form:

$$x(t) = \mathrm{dc}(t) + A(t)\cos\left(\int_0^t 2\pi f(\tau)d\tau + \phi(t)\right). \tag{6}$$

Similar to the operations in (1) and (2), multiplying (6) by $e^{-j\int_0^t 2\pi f(\tau)d\tau}$ yields both instantaneous amplitude $A(t)$ and instantaneous phase $\phi(t)$, so that

$$\begin{aligned} z(t) &= x(t)e^{-j\int_0^t 2\pi f(\tau)d\tau} \\ &= \mathrm{dc}(t)e^{-j\int_0^t 2\pi f(\tau)d\tau} + \left(\frac{A(t)}{2}\right)e^{j\phi(t)} \\ &\quad + \left(\frac{A(t)}{2}\right)e^{-j\left(\int_0^t 4\pi f(\tau)d\tau + \phi(t)\right)}. \end{aligned} \tag{7}$$

From (7), if $z(t)$ is filtered with an ideal LPF with a cutoff frequency $f_c < f_0$, then the filtered signal $z_{\rm lp}(t)$ will be obtained with the same instantaneous amplitude $A(t)$ and phase $\phi(t)$ as provided in (4) and (5). The instantaneous frequency is given by [19] as

$$f(t) = f_0 + \frac{1}{2\pi}\frac{d\phi(t)}{dt}. \tag{8}$$

In the case of variable frequency, the center frequency f_0 is replaced with a variable frequency. We first use a center frequency to estimate the instantaneous frequency within the arbitrarily set frequency band using (8). It is reasonable to expect instantaneous frequencies that are changing, especially if the dynamics are highly TV. Thus, we utilize a subsequent variable frequency approach, which accounts for the possible TV nature of instantaneous frequency within the defined frequency bands to obtain a more precise measurement of instantaneous frequency.

By changing the center frequency followed by using the variable frequency approach of (1) and (6), respectively, as well as the LPF, the signal $x(t)$ will be decomposed into the sinusoid modulations by the CDM technique, as follows:

$$x(t) = \sum_i A_i(t)\cos\left(\int_0^t 2\pi f_i(\tau)d\tau + \phi_i(t)\right) + \mathrm{dc}(t). \tag{9}$$

The instantaneous frequency and amplitude of A_i can be calculated using the Hilbert transform. The entire time–frequency spectrum can be obtained by the calculation of the Hilbert transform of (9) for all time points for the obtained low-pass-filtered frequency components, as described in (3). Therefore, by the combination of the CDM and Hilbert transform, a high TF resolution spectrum and accurate amplitude information can be obtained.

The procedure for the implementation of the CDM or FFCDM on a TFS is summarized next.

1) Design a finite-impulse response (FIR) LPF with the bandwidth and the length of the filter set to F_ω and N_ω, respectively. Set center frequencies as
$$f_{0_i} = (i-1)(2F_\omega), \qquad i = 1, 2, \ldots, \mathrm{int}\left(\frac{f_{\max}}{2F_\omega}\right). \tag{10}$$
where the bandwidth between neighboring center frequencies is $2F_\omega$, and $f_{\max}$ represents the highest signal frequency.
2) Use the FFCDM to extract the dominant frequency within the confined bandwidth and repeat it over the entire frequency band (by incrementing f_{0_i}).
3) Decompose the signal into sinusoidal modulations via the CDM.
4) Calculate the instantaneous frequencies using (8) based on the phase (5) and the instantaneous amplitudes (4) of each sinusoidal modulation component using the Hilbert transform.
5) Obtain the TF representation of the signal using the estimated instantaneous frequencies and amplitudes.

For the VFCDM method, only the center frequencies known as the "backbones" of the FFCDM time–frequency spectrum are considered in subsequent analysis. This approach allows a considerable reduction in computation time since only a few frequencies (those of interest) are analyzed. Once we have an estimate of center frequencies, the LPF cutoff frequency can be made even smaller than the first step of the VFCDM. Design a FIR LPF in which the bandwidth of the filter is set to $F_\nu = F_\omega/2$, and the length of the filter is set to $N_\nu = N_\omega$ along the estimated center frequencies $f_i(t)$. We have previously shown that for the VFCDM, the aforementioned choices of the LPF cutoff frequencies and the length of the filter provide good TFS estimates [16].

Extract more refined amplitude and phase information via steps 3–5. These procedures are used to further improve the performance of the TFS.

B. Extraction of Respiratory Rate

In the following sections, we describe three different methods for extracting respiratory rates. Our proposed method VFCDM will be compared to the CWT and AR modeling approaches in Section III.

1) Extraction of Respiratory Rate Using the VFCDM: Once the TFS is obtained via the VFCDM method as described before, respiratory rates are determined by extracting the frequency component that has the largest amplitude for each time point at the heart rate frequency band, since this component reflects the FM. This is justified since the FM is a form of fluctuation that is reflected in the subfrequency band of a carrier wave, which in our case is the heart rate. To determine frequencies (e.g., respiratory rate) associated with these oscillations, the power spectrum of the FM sequence is calculated and the frequency at which the highest peak occurs is the desired respiratory rate. A TV spectral method can be used in lieu of the power spectrum if the FM time series is nonstationary. The same procedure is also used for extraction of respiratory rate using the AM.

2) Extraction of Respiratory Rates Using CWTs: As recommended by Leonard *et al.* [5]–[7], Addison and Watson [12], [13], and Clifton *et al.* [14], we used a Morlet wavelet with a half-length of five samples at the coarsest scale to estimate the scalogram of the PPG signal. The procedure to extract respiratory rates from the CWT is identical to the VFCDM, as described previously. An important difference between the CWT and CDM methods is that the CWT method employed by Leonard *et al.* [5]–[7], Addison and Watson [12], [13], and Clifton *et al.* [14] essentially selects the best estimate of the breathing rate from the calculated AM and FM estimates. However, they do not explicitly detail how this selection is done. Hence, for comparison purposes, we divided the results into two separate categories: results from CWT-AM and results from CWT-FM calculations.

3) Extraction of Respiratory Rates Using AR Modeling: Fleming and Tarassenko have recently developed an AR modeling approach to respiratory rate estimation [15], which models the PPG signal using the Burg algorithm [20]. As such, the PPG signal $x(n)$, where n denotes the number of samples, can be

modeled as a weighted sum of past $x(n)$ values in the following manner:

$$x(t) = -\sum_{k=1}^{p} a(k)x(n-k) + e(n). \tag{11}$$

The error $e(n)$ is assumed to be normally distributed with zero mean and a variance σ^2, and can be seen as a driving input to the system, in which case the transfer function of the system can be written as follows:

$$H(z) = \frac{z^p}{(z-z_1)(z-z_2)\cdots(z-z_p)}. \tag{12}$$

The aforementioned transfer function has p complex conjugate poles and no finite zeros. The resonant frequency of each spectral peak is given by the phase angle of that pole as

$$f = \frac{\theta}{2\pi\Delta t}. \tag{13}$$

Here, Δt is the sampling interval of the PPG signal. After calculating the separate resonant frequencies corresponding to every pole, the specific breathing pole is recognized by comparing the magnitudes of the poles, since it is expected that the breathing poles have the highest magnitudes. Only those candidates are chosen that have resonant frequencies in the possible breathing range. Out of these, only that breathing pole is chosen which has the smallest phase angle. For specific details of the preconditioning and pole-selection algorithms, see [15].

C. Data Acquisition

Data were collected on 15 healthy subjects (seven female and eight male, mean age 21 ± 1.2 years) using a MP506 pulse oximeter (Nellcor Oximax, Boulder, CO) reusable sensor (Durasensor DS-100A), which incorporates a conditioning circuit and has an analog output of 4.864 kHz. No subject had cardiorespiratory or related pathologies. Data were collected in the upright and supine positions, and the sensor was attached to the subjects' left index or middle finger. The subjects were instructed to breathe at a constant rate according to a timed beeping sound, i.e., to start an inspiration whenever they heard a beep sound programmed at a chosen frequency. The data were collected for breathing frequencies ranging from 0.2 to 0.6 Hz at an increment of 0.1 Hz. The subjects were given some time to practice breathing at the beeping rate. Three minutes of data were collected for each frequency for each subject, for both upright and supine positions. A true breathing signal was also acquired via the Respitrace system, which uses inductive plethysmography to provide calibrated voltage outputs corresponding to rib cage and abdominal compartment volume changes. The Respitrace system is cumbersome to use since inductive bands are worn over the rib cage and abdomen, and the system requires calibration for each subject and it is more expensive than a pulse oximeter. Since in this study we are merely interested in the rate of respiration and not the amplitude, a simple FFT and/or manual counting of the number of peaks can be done on the Respitrace signal to obtain the frequency of oscillation. Data acquisition was done using the ADInstruments PowerLab/4Sp data acquisition system and routed into the PC via a universal serial bus (USB) port. Chart v4.2.2 software (ADInstruments, Colorado Springs, CO) was used to sample the analog signal at 200 Hz.

D. Data Analysis

Three minutes of data sampled at 200 Hz were low-pass-filtered to 10 Hz, and then downsampled to 20 Hz. We performed the extraction of the respiratory rate on every 1-min segment of PPG signal, and then the data were shifted by every 10 s for the entire 3 min of recordings, i.e., each 1-min dataset had a 50 s overlap. Hence, for each 3-min segment, we had 13 1-min segments to analyze for all methods to be compared. Thus, 3 min of data were sufficiently long to test the efficacy of each method but not too long in duration to fatigue the subjects as their task was to breathe on cue with a metronome. For the CDM and CWT methods, for every 1-min segment, the initial and final 5 s of the TFS were not considered because the TFS has an inherent end effect that could create false variability. The filter parameters of the VFCDM were set to $F_\omega = 0.03$ Hz, $F_\nu = 0.015$ Hz (both are normalized frequencies), and $N_\omega = 64$. Fig. 2 and Section III illustrate how $F_\omega = 0.03$ Hz was derived. We have previously shown that the parameter $F_\nu = F_\omega/2$, and that N_ω is chosen to be approximately half the data length [16].

III. Results

An example of a representative 1-min segment of PPG data and its VFCDM time–frequency spectrum when the subject was breathing at a rate of 0.2 Hz (12 breaths/min) is shown in Fig. 1(a) and (b), respectively. As shown in Fig. 1(a), the periodic oscillations of the PPG signal are nearly periodic, and thus, our use of the CDM approach to model the signal as per (6) is appropriate. Note especially the primary FM seen around 1.5 Hz that corresponds to the heart rate (90 beats/min); other higher frequency peaks (e.g., 3 Hz, 4.5 Hz, etc., are harmonics of 1.5 Hz). Fig. 1(c) shows the extracted FM time series at each time point from the TFS shown in Fig. 1(b), and its subsequent power spectrum is shown in the Fig. 1(d). The largest peak in this power spectrum is the 0.2 Hz, which corresponds correctly to the breathing rate.

The Nyquist frequency in this case is 10 Hz, but we only consider the frequency range from 0.15 to 0.7 Hz. In some cases, peaks were seen at frequencies greater than 0.7 Hz, and they were found to be mainly due to measurement artifacts and harmonics of the $f < 0.7$ Hz dynamics. As a breathing rate more than 0.7 Hz is unrealistic, we ignore the range of frequencies (i.e., $f > 0.7$ Hz) when looking for the highest peaks. Furthermore, no method was able to provide accurate results when the true breathing frequencies were greater than 0.7 Hz. In addition, we excluded breathing rates that are lower than 0.15 Hz since dynamics pertaining to the sympathetic tone are known to be active in the frequency range between 0.04 and 0.15 Hz. For example, if a subject's breathing rate is 0.3 Hz with the sympathetic tone highly innervated, then the largest peak may be located anywhere in the frequency band of 0.04–0.15 Hz instead of the expected respiratory rate peak at 0.3 Hz. It should be noted, however, that the VFCDM method is accurate

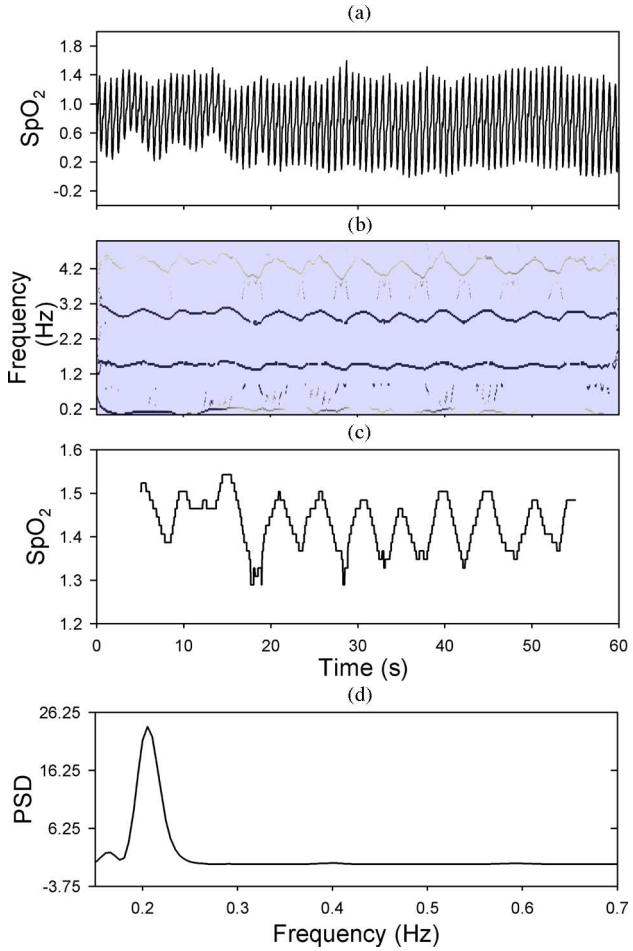

Fig. 1. (a) Representative pulse oximeter signal. (b) Estimated instantaneous frequencies using VFCDM with prominent frequency oscillations seen near heart rate (1.5 Hz). (c) FM sequence extracted from the pulse ridge in the time–frequency plot. (d) PSD of the FM signal. It is clear that the highest peak is obtained at 0.2 Hz, which is same as the breathing frequency (12 beats/min).

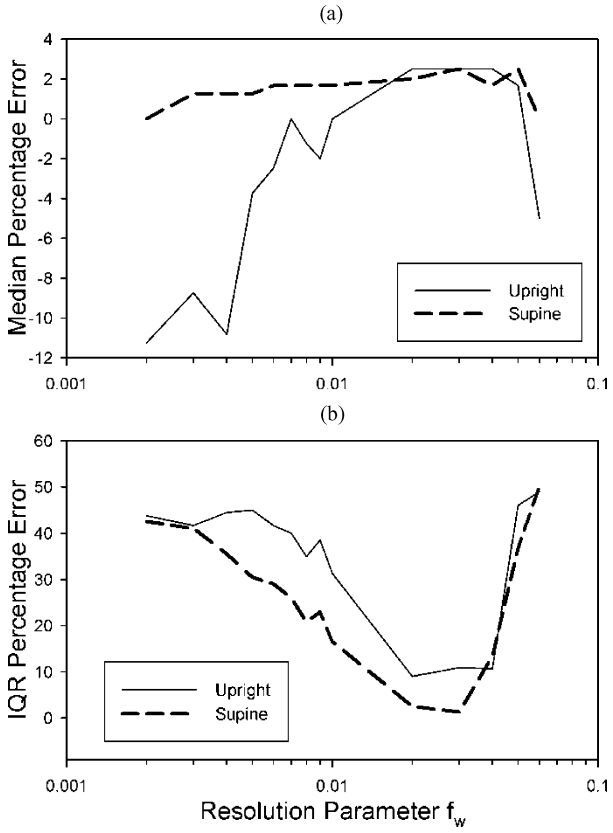

Fig. 2. Semilog plots showing trend of (a) median and (b) IQR of error percentage as a function of the resolution parameter for the VFCDM-FM method. The best results were obtained with regard to both accuracy and spread of error across subjects, frequencies, and positions using a parameter value of 0.03.

even for respiratory rates lower than 0.15 Hz, but we do not provide comprehensive results for breathing rates lower than this since the peaks associated with sympathetic tone could confound detection at higher breathing rates.

For a complete comparison of all these methods, it is necessary to look at differences in results across subjects, across time, across different body positions (supine and upright breathing positions), and across true breathing rate. In order to do this in an effective manner, we divide the results into two broad categories, supine and upright. For each of these categories, percentage detection errors were found for each frequency for all subjects using the four different methods. The percentage error is calculated as follows:

$$\%\text{Error} = \left(\frac{\hat{R} - R}{R}\right) 100. \tag{14}$$

Where $\hat{R}$ denotes the detected breathing rate and R is the true breathing rate. For every subject, we obtained 13 detections (from 3 min recordings with 1 min data analysis window shifted in time by 10 s) for each breathing frequency. The median and interquartile range (IQR) (difference between the 25th and 75th percentile) of the percentage detection errors of these 13 detections were compiled for all four methods for every frequency for every subject. The median value provides an estimate of the accuracy of the method while the IQR gives an estimate of the ability of the algorithm to track the frequency across time (within the data duration of 3 min) for every subject. Hence, a median value that is close to zero would indicate good accuracy of the method studied. Similarly, the smaller the IQR, the better the rate tracking ability or repeatability of the method. These two statistics were compared across the entire population (15 subjects).

It is instructive to observe the change in accuracy and consistency of detection with the variation of the principal resolution-determining parameter for the VFCDM method, i.e., the F_ω. Fig. 2(a) shows the variation of the median detection error percentage as the F_ω parameter is varied from 0.002 to 0.06 Hz for the supine (dashed line) and upright (solid line) positions. It can be seen that the median error starts from a high negative value and gradual improves to a little above 0% for both body positions before increasing in magnitude again. Similarly, Fig. 2(b) shows the variation of the spread (as measured by the IQR of the percentage error) as the resolution parameter increases over the same range as previously for the supine (solid line) and upright (dotted) positions. Again, it can be seen that the most

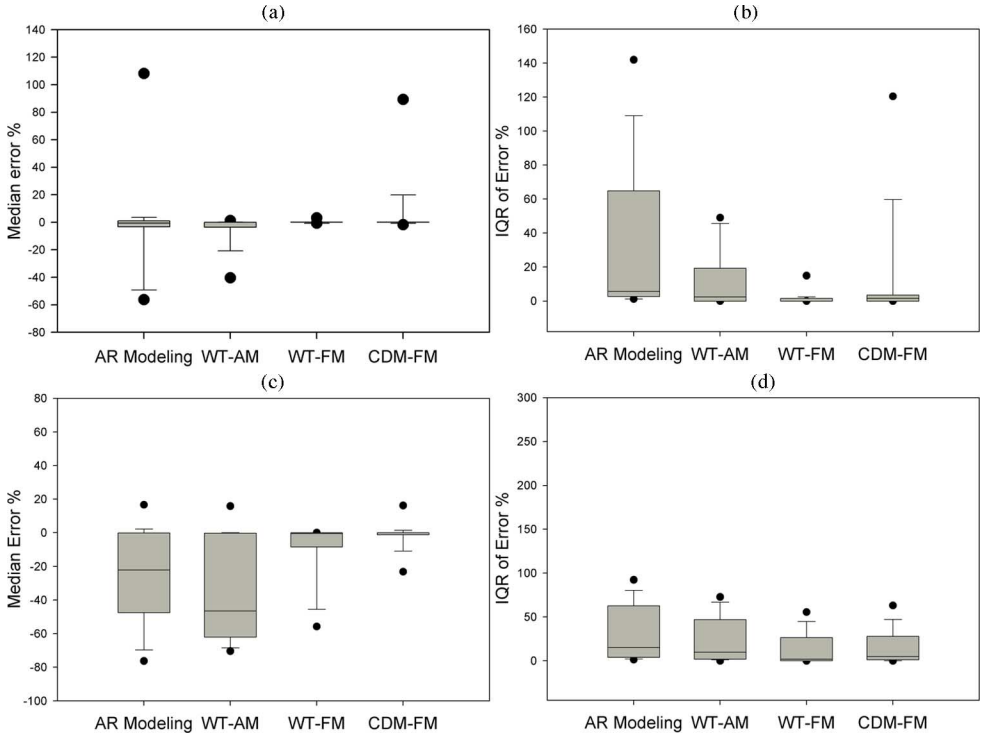

Fig. 3. (Left panels) Median errors and (right panels) IQR errors for the supine position. The top row (a) and (b) are for low breathing frequencies (0.2 and 0.3 Hz), and the bottom row (c) and (d) are for high frequencies (0.4–0.6 Hz). Filled circles above and below each bar graph represent the 95th and 5th percentiles, respectively.

desirable IQR values are obtained for F_ω values of 0.02–0.04 for both body positions. Note that the dramatic decrease in IQR variables from F_ω is 0.01–0.03 Hz more than compensates for the slight decrease in median errors (a measure of the accuracy) over the same range. For the sake of consistency, we chose a value of $F_\omega = 0.03$ Hz for our method.

Figs. 3 and 4 show the accuracy and repeatability of each method as a function of true breathing rate for the supine (Fig. 3) and upright (Fig. 4) positions. For tabulating the results, we grouped the results for 0.2–0.3 Hz together and designated them as the LF breathing rates. Likewise, the results for 0.4–0.6 Hz breathing rates were lumped together and designated as the HF breathing rates. Statistical testing (using an ANOVA on ranks) was done to see if there were significant differences between the medians for the four different methods. In addition, a Brown–Forsythe test was used to compare the variances across the population. Since the percentage errors obtained were found to be not normally distributed, we used median, IQR, and nonparametric tests like ANOVA on ranks, and the Brown–Forsythe test instead of the mean, standard error, and parametric tests such as one-way ANOVA or Levene test (for variance).

Figs. 3 and 4 show the subjects' variation of the median (left panels) and IQR (right panels) of percentage detection error for the supine and upright positions, respectively, in the form of box plots. The top and bottom panels of Figs. 3 and 4 represent results for the LF and HF breathing rates, respectively. The lower boundary of the box closest to zero indicates the 25th percentile, a line within the box marks the median, and the upper boundary of the box farthest from zero indicates the 75th percentile. Whiskers (error bars) above and below the box indicate the 90th and 10th percentiles. Hence, the gray area of the box is an indication of the spread, i.e., the variation in median error (or IQR), across the population. These figures indicate how well the algorithms perform across the entire population. Solid circles represent the 5th and 95th percentiles. The top panels of Tables I and II summarize these measures of accuracy (median) and "repeatability across time" (IQR), respectively, by tabulating the median and IQR of these statistics across the population for both supine and upright positions. The bottom panels of Tables I and II provide a summary of statistical analysis comparing the performance of the four methods to each other.

The AR model approach is the least accurate followed by CWT-AM, CWT-FM, and VFCDM when we consider all body positions and all breathing frequencies. For LF breathing rates, there was no significant difference in the median error between all four methods for both body positions as they were all accurate. However, the variances of the median values as determined by the IQR of median error are significantly lower for both VFCDM and CWT-FM than for either CWT-AM or AR model approaches.

In general, the median error is larger in HF than LF breathing rates. For HF breathing rates, the median error is lowest for VFCDM, followed by CWT-FM, CWT-AM, and AR model for both body positions. While there is no significant difference in the variance between VFCDM and CWT-FM, both methods have significantly less variance than either CWT-AM or AR model. Thus, gauging the accuracy as defined by the median

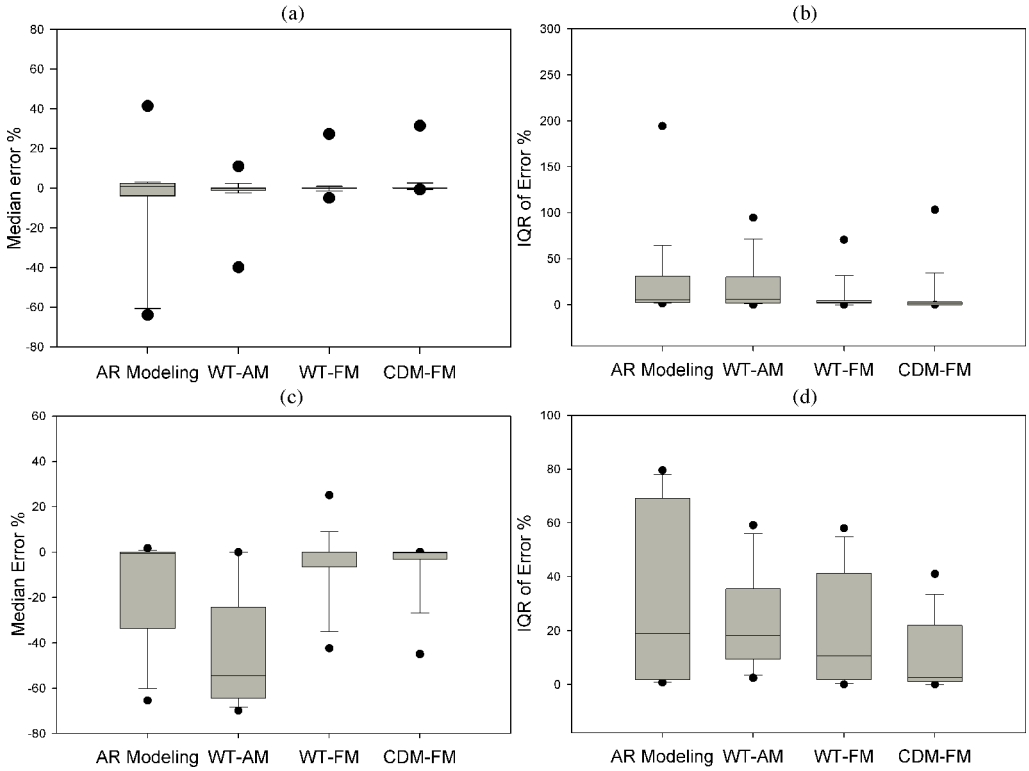

Fig. 4. (Left panels) Median errors and (right panels) IQR errors for the upright position. The top row (a) and (b) are for low breathing frequencies (0.2 and 0.3 Hz) and the bottom row (c) and (d) are for high frequencies (0.4–0.6 Hz). Filled circles above and below each bar graph represent the 95th and 5th percentiles, respectively.

TABLE I
(TOP) ACCURACY AS DETERMINED BY MEDIAN ERRORS AND IQR OF MEDIAN ERRORS FOR BOTH BODY POSITIONS. (BOTTOM) STATISTICAL SIGNIFICANCE AMONG THE FOUR METHODS FOR BOTH BODY POSITIONS

Position	True Breathing Rate (Hz)	AR Modeling		CWT-AM		CWT-FM		VFCDM-FM	
		Median of *median error (%)*	IQR of *median error (%)*	Median of *median error (%)*	IQR of *median error (%)*	Median of *median error (%)*	IQR of *median error (%)*	Median of *median error (%)*	IQR of *median error (%)*
Upright	LF(0.2-0.3Hz)	0.81	5.12	0.00	1.12	0.00	0.07	0.00	0.07
	HF(0.4-0.6 Hz)	-0.67	27.29	-54.47	39.02	0.00	4.98	-0.39	2.52
Supine	LF(0.2-0.3Hz)	-0.57	3.69	0.00	3.05	0.00	0.00	0.00	0.0977
	HF(0.4-0.6 Hz)	-22.14	43.85	-46.53	61.50	-0.39	1.37	0.00	1.12

	LF		HF	
	Medians	Variances	Medians	Variances
Upright	None	WT-FM vs WT-AM VFCDM-FM vs WT-AM	WT-FM vs WT-AM WT-FM vs AR model WT-FM vs VFCDM-FM VFCDM-FM vs WT-AM AR model vs WT-AM	AR model vs WT-AM AR model vs VFCDM-FM WT-FM vs WT-AM VFCDM-FM vs WT-AM
Supine	None	AR model vs WT-AM WT-FM vs WT-AM VFCDM-FM vs WT-AM	VFCDM-FM vs WT-AM VFCDM-FM vs AR Model VFCDM-FM vs WT-FM WT-FM vs WT-AM WT-FM vs AR Model AR model vs WT-AM	AR model vs WT-AM WT-FM vs WT-AM VFCDM-FM vs WT-AM

errors and their variances, as shown in the left panels of Figs. 3 and 4, and presented numerically in the top panel of Table I, we observe that for both LF and HF breathing rates, VFCDM consistently provides the lowest median errors and variance values.

Repeatability or consistency of the four methods is shown in the right panels of Figs. 3 and 4, and numerically in the top panel of Table II. In general, the ability of the methods to provide consistent results is especially excellent (highest) for both the CWT-FM and VFCDM methods, for both LF and HF breathing

TABLE II
(TOP) REPEATABILITY ACROSS TIME AS DETERMINED BY MEDIAN OF IQR ERRORS AND IQR OF IQR ERRORS FOR BOTH BODY POSITIONS. (BOTTOM) STATISTICAL SIGNIFICANCE AMONG THE FOUR METHODS FOR BOTH BODY POSITIONS

Position	True Breathing Rate (Hz)	AR Modeling		CWT-AM		CWT-FM		VFCDM-FM	
		Median of *IQR error* (%)	IQR of *IQR error* (%)	Median of *IQR error* (%)	IQR of *IQR error* (%)	Median of *IQR error* (%)	IQR of *IQR error* (%)	Median of *IQR error* (%)	IQR of *IQR error* (%)
Upright	LF(0.2-0.3Hz)	5.33	15.84	6.51	26.21	2.50	3.25	1.64	3.27
	HF(0.4-0.6 Hz)	18.91	66.84	18.29	24.59	10.64	39.16	2.47	19.77
Supine	LF(0.2-0.3Hz)	5.69	61.96	2.44	16.78	1.62	1.64	1.64	3.27
	HF(0.4-0.6 Hz)	15.16	55.52	9.80	41.70	1.96	25.49	4.88	25.25

	LF		HF	
	Medians	Variances	Medians	Variances
Upright	VFCDM-FM vs WT-AM VFCDM-FM vs AR Model VFCDM-FM vs WT-FM WT-FM vs WT-AM WT-FM vs AR Model	None	VFCDM-FM vs AR Model VFCDM-FM vs WT-AM VFCDM-FM vs WT-FM	WT-FM vs AR model VFCDM-FM vs AR Model VFCDM-FM vs WT-AM VFCDM-FM vs WT-FM
Supine	VFCDM-FM vs AR Model VFCDM-FM vs WT-FM WT-FM vs WT-AM WT-FM vs AR Model AR model vs WT-AM	AR model vs WT-AM AR model vs WT-FM AR model vs VFCDM-FM WT-FM vs WT-AM	VFCDM-FM vs WT-AM VFCDM-FM vs AR Model VFCDM-FM vs WT-FM WT-FM vs WT-AM WT-FM vs AR Model AR model vs WT-AM	None

rates and body positions. As with the accuracy results, the repeatability is also better for the LF than for the HF breathing rates for all four methods. Both CWT-FM and VFCDM provide significantly more repeatable results than either CWT-AM or AR model.

IV. DISCUSSION

In this study, we demonstrated the accuracy of a novel approach to extract respiratory rates from pulse oximeter recordings. The method was shown to be accurate for widely varying breathing rates, and can be implemented in real time. We compared our method to both wavelet and AR-based approaches since these two techniques are among the most accurate algorithms to date [15]. Overall, our method based on the use of VFCDM to extract FM signals followed by the power spectrum to extract the respiratory rate is the most accurate and with the fastest computational time than any of the methods compared for both supine and upright positions. The continuous wavelet approach using either the FM or AM signals fared better than the AR method for both body positions at the expense of larger computational time.

Estimation of respiratory rate is important in monitoring of patients, whether at home or in a hospital facility. Due to the highly labor-intensive and sometimes invasive nature of accurate respiratory rate estimation, we aimed to develop an algorithm to extract respiration rate from the pulse oximeter, a noninvasive, easy-to-use device intended for measurement of oxygen saturation level. The work by Addison *et al.* [5]–[7], Shelley *et al.* [8], Addison and Watson [12], [13], and Clifton *et al.* [14] is noteworthy since it is one of the first studies to use a time–frequency approach, as opposed to the time domain approaches using filtering methods [9]–[11], [21], [22] to estimate respiratory rates using the pulse oximeter. A time–frequency method is ideally suited for studying the pulse oximeter signal because of the inherent nonstationarity in the respiratory rate. In addition, a filtering approach usually involves tuning of a number of parameters that pose a problem when signal characteristics vary from subject to subject. While Fleming and Tarassenko [15] do mention a decrease in accuracy when the AR modeling approach is used on 30-s segments (real-time implementation) instead of 5-min segments, we found that this decrease was far greater than that obtained with time–frequency approaches.

Our method is similar to the work by Addison *et al.* [5]–[7], Addison and Watson [12], [13], and Clifton *et al.* [14] in that we also estimate the TFS of the PPG signal, but differs from them since we only use the FM signals and not both AM and FM signals, and a different TFS estimation method is used. The reason why Addison *et al.* used both AM and FM signals is that the accuracy of the extracted respiratory rate was better with FM in some cases while the AM provided better results in other instances [5]–[7], [12]–[14]. We also found that this was the case with our results using the wavelet approach. They suggested the use of an *ad hoc* approach to determine when to select either the AM or FM results; however, the details on implementation of this decision procedure are not available in any of their published works.

Instead of a wavelet approach, we used our recently developed VFCDM method that was shown to provide one of the highest time–frequency resolutions [16]–[18]. Hence, we anticipated that using this approach in estimating the TFS would yield better results in respiratory rate estimation than the wavelet approach used by Addison *et al.* [5]–[7], Addison and Watson [12], [13], and Clifton *et al.* [14]. While we are also able to extract respiratory rate from both AM and FM signals, we found that the results on the AM signals were not as reliable as the FM signals. In a way, this is a good news since we do not have to use some complicated decision scheme to determine when

to use the results of AM or FM. As shown in both Figs. 3 and 4, and Tables I and II, the respiratory rate detection using the FM signals derived from the wavelet method provided better results than AM signals in most cases for both body positions. Thus, similar to our approach, a case can be made that the wavelet method can also use only the FM signals to extract the respiratory rates. Even with such a scheme, the VFCDM approach provides better estimates of the respiratory rates in most cases.

Another advantage of our algorithm is that the estimation of TFS is considerably faster than the wavelet method. The average time to calculate the respiration frequency using the VFCDM method was found to be around 0.3 s, while using the Wavelet method took 2 s on average (programs running on MATLAB R2007b). This means that a real-time implementation of the algorithm would be considerably faster and easier using the VFCDM method. The AR spectral method was the fastest as it took 0.1 s on average using MATLAB, and this computation time includes the time needed to calculate the model order based on an initial model order selection of 50.

In contrast to the findings by Leonard *et al.* [7], we did find the existence of rate-dependent error in detection of breathing rate. This is probably because Leonard *et al.* used longer segments of the PPG signal in their study (180 s compared to 60 s for this study). In addition, the study in [7] compared detection accuracies for breathing rates only as high as 27 breaths/min (0.45 Hz). In this study, it was observed that for both wavelet and VFCDM methods, and for both supine and upright conditions, detection of the respiratory frequency became less accurate with increase in actual breathing rate. However, for the upright condition, the VFCDM method provides better respiration rate estimate than the WT-FM or WT-AM methods. Note that the most accurate results were obtained for respiration frequencies 0.2 and 0.3 Hz. It should be noted that the normal range of breathing rate falls in this range, and breathing rates higher than 0.5 Hz are rare. Hence, we anticipate that this method of breathing frequency extraction should perform quite well in most cases. In fact, for very high breathing rates, the method would at least serve to give a clear indication of deviation from normal frequency, even if it is not able to estimate the frequency itself with very high accuracy.

We can speculate about the reason for less accurate results with higher respiratory rates seen in our study with all algorithms tested. Detection of both AM and FM requires persistent oscillations for several cycles, but with faster respiratory rates, this condition may not hold. In addition, with faster breathing rates, the amplitudes of AM or FM become less, and thus, it becomes more difficult to detect them. Thus, a higher resolution-based TFS method such as the VFCDM is required to work better with higher respiratory rates; such was the case in our paper.

A. Limitations

We have limited our study to healthy subjects to demonstrate the feasibility of the proposed approach. Detection of accurate respiratory rates may not be optimal for subjects with certain cardiovascular diseases that increase sympathetic tone. For example, subjects with a pacemaker or on heart rhythm changing medications may lead to less accurate respiratory rate detection using our approach. For all other subjects, however, we believe that the method proposed in this paper is feasible.

Literature also supports our claim. A work by Clifton *et al.* [14] has reported accurate respiratory rate detection in subjects with respiratory problems, as well as in subjects under general anesthesia and recovering from it, using the same CWT method as compared in our paper. In addition, a work by Leonard *et al.* [7], and a work by Fleming and Tarassenko [15] have reported accurate respiratory rate detection in children with spontaneous breathing using the CWT and AR modeling approaches, respectively. Thus, given the fact that we have used the same CWT and AR modeling methods, as in the aforementioned studies, for comparisons to our method, we believe that our method will be as accurate in healthy young and adult subjects with spontaneous breathing, subjects with respiratory problems, and in patients during anesthesia and post anesthesia. Furthermore, for most healthy and unhealthy subjects described before, their spontaneous breathing rates fell within 0.2–0.4 Hz [14], and given our accurate detection in these rates, it is not unreasonable to assume that our method will be just as accurate or better than the case of spontaneous breathing rates.

The Mayer wave oscillation often seen in spontaneous arterial pressure has a characteristic frequency of $\sim$0.1 Hz in humans, and is enhanced during the state of sympathetic activation [23]. For this reason, we did not provide results on respiratory rates lower than 0.15 Hz, since the peaks associated with sympathetic tone (0.04–0.15 Hz) could confound detection at higher breathing rates. Note that spectral peaks in the range of 0.04–0.15 Hz arise due to the actions of the sympathetic tone [24] or Mayer waves at $\sim$0.1 Hz [23]; thus, detection of respiratory rates will be suboptimal if a subject has events that elevate the sympathetic activities or the presence of Mayer waves such that their spectral peaks are larger than the respiratory peak.

In this paper, we tested the performance of the VFCDM method against metronome breathing and not spontaneous breathing. The metronome breathing allowed us to estimate near real-time performance of the algorithm as our results are based on 1-min data segments that are shifted every 10 s. In our opinion, spontaneous breathing masks give the true performance of the algorithms since the results in the literature are often reported based on the averaged respiratory rates as they vary over the duration of 3 min [5]–[7], [12]–[14]. Thus, rather than comparing the results based on the averaged respiratory rate over the entire duration of the data segment, we believe that our choice of reporting the results based on each 10 s shift provides better assessment of the algorithms as well as their near real-time performances. In addition, we can better gauge the true performance of the algorithms since the subjects are breathing at a frequency equal to or very close to the "metronomic" respiratory rate.

In summary, we demonstrated a real-time realizable and consistently accurate approach to extract respiratory rates from direct recordings of the pulse oximeter using the VFCDM approach. The CWT-FM method also provides good results but its computational speed is about seven times slower than VFCDM.

The novelty of either VFCDM or CWT-FM not only resides in our ability to extract accurate respiratory rates, but also in the fact that we can obtain an additional clinically important parameter from the pulse oximeter. Thus, with the pulse oximeter, we can obtain not only the oxygen saturation levels and heart rate, but also the respiratory rates. We believe that this is important because the pulse oximeter is a proven technology that is widely accepted in practice, and the ability to extract multiple vital signs from a single sensor will facilitate enhancements not only from a technical standpoint but, most importantly, from the point of patients' comfort, since they do not have to wear multiple sensors to obtain the same vital sign information.

REFERENCES

[1] A. C. Guyton, *Human Physiology and Mechanisms of Disease*, 4th ed. Philadelphia, PA: Saunders, 1987.

[2] M. Younes, "Role of respiratory control mechanisms in the pathogenesis of obstructive sleep disorders," *J. Appl. Physiol.*, vol. 105, pp. 1389–1405, Nov. 2008.

[3] T. Rantonen, J. Jalonen, J. Gronlund, K. Antila, D. Southall, and I. Valimaki, "Increased amplitude modulation of continuous respiration precedes sudden infant death syndrome-detection by spectral estimation of respirogram," *Early Hum. Dev.*, vol. 53, pp. 53–63, Nov. 1998.

[4] M. Hasselgren, M. Arne, A. Lindahl, S. Janson, and B. Lundback, "Estimated prevalences of respiratory symptoms, asthma and chronic obstructive pulmonary disease related to detection rate in primary health care," *Scand. J. Prim. Health Care*, vol. 19, pp. 54–57, Mar. 2001.

[5] P. Leonard, T. F. Beattie, P. S. Addison, and J. N. Watson, "Standard pulse oximeters can be used to monitor respiratory rate," *Emerg. Med. J.*, vol. 20, pp. 524–525, Nov. 2003.

[6] P. Leonard, N. R. Grubb, P. S. Addison, D. Clifton, and J. N. Watson, "An algorithm for the detection of individual breaths from the pulse oximeter waveform," *J. Clin. Monit. Comput.*, vol. 18, pp. 309–312, Dec. 2004.

[7] P. A. Leonard, D. Clifton, P. S. Addison, J. N. Watson, and T. Beattie, "An automated algorithm for determining respiratory rate by photoplethysmogram in children," *Acta Paediatr.*, vol. 95, pp. 1124–1128, 2006.

[8] K. H. Shelley, A. A. Awad, R. G. Stout, and D. G. Silverman, "The use of joint time frequency analysis to quantify the effect of ventilation on the pulse oximeter waveform," *J. Clin. Monit. Comput.*, vol. 20, pp. 81–87, Apr. 2006.

[9] K. Nakajima, T. Tamura, and H. Miike, "Monitoring of heart and respiratory rates by photoplethysmography using a digital filtering technique," *Med. Eng. Phys.*, vol. 18, pp. 365–372, 1996.

[10] L. Nilsson, A. Johansson, and S. Kalman, "Monitoring of respiratory rate in postoperative care using a new photoplethysmographic technique," *J. Clin. Monit. Comput.*, vol. 16, pp. 309–315, 2000.

[11] L. Nilsson, A. Johansson, and S. Kalman, "Respiration can be monitored by photoplethysmography with high sensitivity and specificity regardless of anaesthesia and ventilatory mode," *Acta Anaesthesiol. Scand.*, vol. 49, pp. 1157–1162, 2005.

[12] P. S. Addison and J. N. Watson, "Secondary wavelet feature decoupling (SWFD) and its use in detecting patient respiration from the photoplethysmogram," in *Proc. 25th Annu. Int. Conf. IEEE Eng. Med. Biol. Soc.*, 2003, vol. 3, pp. 2602–2605.

[13] P. S. Addison and J. N. Watson, "Secondary transform decoupling of shifted nonstationary signal modulation components: Application to photoplethysmography," *Int. J. Wavelets Multiresolution Inf. Process.*, vol. 2, pp. 43–57, 2004.

[14] D. Clifton, J. Douglas, P. Addison, and J. Watson, "Measurement of respiratory rate from the photoplethysmogram in chest clinic patients," *J. Clin. Monit. Comput.*, vol. 21, pp. 55–61, 2007.

[15] S. G. Fleming and L. Tarassenko, "A comparison of signal processing techniques for the extraction of breathing rate from the photoplethysmogram," *Int. J. Biomed. Sci.*, vol. 2, pp. 232–236, 2007.

[16] H. Wang, K. Siu, K. Ju, and K. H. Chon, "A high resolution approach to estimating time–frequency spectra and their amplitudes," *Ann. Biomed. Eng.*, vol. 34, pp. 326–338, Feb. 2006.

[17] K. L. Siu, B. Sung, L. C. Moore, A. Birzgalis, and K. H. Chon, "Very low frequency modulation in renal autoregulation," in *Proc. Conf. Proc. IEEE Eng. Med. Biol. Soc.*, 2006, vol. 1, pp. 771–774.

[18] Y. Zhong, K.-M. Jan, and K. H. Chon, "Frequency modulation between low- and high-frequency components of the heart rate variability spectrum," *Biomed. Tech./Biomed. Eng.*, vol. 51, pp. 251–254, 2006.

[19] A. Monti, C. Medigue, and L. Mangin, "Instantaneous parameter estimation in cardiovascular time series by harmonic and time-frequency analysis," *IEEE Trans. Biomed. Eng.*, vol. 49, no. 12, pp. 1547–1556, Dec. 2002.

[20] S. W. Marple, *Digital Spectral Analysis with Applications*. Englewood Cliffs, NJ: Prentice-Hall, 1987.

[21] A. Johansson, P. A. Oberg, and G. Sedin, "Monitoring of heart and respiratory rates in newborn infants using a new photoplethysmographic technique," *J. Clin. Monit. Comput.*, vol. 15, pp. 461–467, Dec. 1999.

[22] W. S. Johnston and Y. Mendelson, "Investigation of signal processing algorithms for an embedded microcontroller-based wearable pulse oximeter," in *Proc. 28th Annu. Int. Conf. IEEE Eng. Med. Biol. Soc. (EMBS 2006)*, pp. 5888–5891.

[23] C. Julien, "The enigma of Mayer waves: Facts and models," *Cardiovasc. Res.*, vol. 70, pp. 12–21, Apr. 1, 2006.

[24] "Heart rate variability: Standards of measurement, physiological interpretation and clinical use. Task force of the European society of cardiology and the North American society of pacing and electrophysiology," *Circulation*, vol. 93, pp. 1043–1065, Mar. 1, 1996.

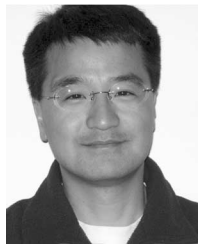

Ki H. Chon (SM'08) received the B.S. degree in electrical engineering from the University of Connecticut, Storrs, the M.S. degree in biomedical engineering from the University of Iowa, Iowa City, and the M.S. degree in electrical engineering and the Ph.D. degree in biomedical engineering from the University of Southern California, Los Angeles.

For three years, he was a National Institute of Health (NIH) Postdoctoral Fellow at the Harvard-Massachusetts Institute of Technology (MIT) Division of Health Science and Technology. For one year, he was a Research Assistant Professor in the Department of Molecular Pharmacology, Physiology, and Biotechnology, Brown University, Providence, RI. For four years, he was an Assistant and an Associate Professor in the Department of Electrical Engineering, City College, City University of New York. He is currently a Professor in the Department of Biomedical Engineering, State University of New York (SUNY) Stony Brook, Stony Brook. He is currently an Associate Editor of the *International Journal of Bioelectromagnetism*. His current research interests include medical instrumentation, biomedical signal processing, and identification and modeling of physiological systems.

Prof. Chon is currently an Associate Editor of the IEEE TRANSACTIONS ON BIOMEDICAL ENGINEERING.

Shishir Dash received the B.Tech. degree in instrumentation engineering from the Indian Institute of Technology Kharagpur, Kharagpur, India. He is currently working toward the Ph.D. degree in the Department of Biomedical Engineering, SUNY Stony Brook, Stony Brook.

His current research interests include cardiovascular dynamics, and linear and nonlinear signal processing of biological signals such as R-R interval time series, and oxygen saturation.

Kihwan Ju received the M.S. degree in electrical engineering from Yonsei University, Seoul, Korea, and the Ph.D degree from the School of Science and Technology, Keio University, Minato, Japan.

He was a Research Associate with the School of Science and Technology, and Sports Medicine Research Center in the School of Medicine, Keio University. He was a a Research Associate Professor in the Department of Physiology, The University of Tokyo and the Institute of Bio-Cybernetics. He was a Research Scientist at the City University of New York. He is currently the Research Director of the Institute of Bio-Cybernetics, and a Research Scientist in the Department of Biomedical Engineering, State University of New York (SUNY) Stony Brook, Stony Brook. His current research interests include system modeling of integrative physiology in the human and genetic-targeted animal model, design of medical instrument, and biomedical signal processing.